NEAR-INFRARED AND OPTICAL SPECTROSCOPY OF FSC 10214+4724[1]

B. T. SOIFER, J. G. COHEN, L. ARMUS, K. MATTHEWS, G. NEUGEBAUER, AND J. B. OKE
Palomar Observatory, Caltech, Pasadena, CA 91125
Received 1994 October 11; accepted 1995 February 3

ABSTRACT

New infrared and optical spectroscopic observations, obtained with the W. M. Keck Telescope, are reported for the highly luminous infrared source FSC 10214+4724. The rest frame optical spectrum shows new emission lines of [Ne III], [Ne V], [O I], [O II], [S II], and He$^+$, while the rest frame ultraviolet spectrum shows new lines of O IV] + Si IV, N III], N IV], Si II, Ne IV, and possibly N II and [Ne III], as well as clearly showing that Lyα is self-absorbed. The emission-line spectrum is most characteristic of a Seyfert 2 nucleus. The preponderance of spectroscopic evidence strengthens the case for a dust-enshrouded AGN powering much or most of the observed luminosity. The various spectral lines lead to a wide range in the inferred reddening and ionization parameter for this system, suggesting that we are viewing several environments through differing extinctions.

Subject headings: galaxies: individual (FSC 10214+4724) — galaxies: Seyfert

1. INTRODUCTION

The *IRAS* source FSC 10214+4724 has been the subject of intensive observational scrutiny since it was found to be at a redshift of 2.286, making it among the most luminous objects in the universe (Rowan-Robinson et al. 1991). Its prodigious luminosity is matched only by the most luminous quasars. It is likely that an AGN is the main source of power in this object, though star formation probably contributes significantly to the luminosity. The AGN origin of much of the luminosity is suggested by the Seyfert 2 spectral classification (Elston et al. 1994) and the very large ratio of luminosity to gas mass ($L/M \sim 10^3$ in solar units), while evidence for a significant contribution from star formation comes from the abundant (10^{11} $M_\odot$) supply of molecular gas in the system (Brown & Vanden Bout 1991; Solomon, Downes, & Radford 1992) and the extended nature of the Hα emission (Matthews et al. 1994).

Complicating the interpretation of this system is the possibility that a nearby companion source, 1″.5 to the north of the emission-line system, could in fact be an intervening galaxy that acts as a gravitational lens (Matthews et al. 1994; Elston, et al. 1994). This would explain the morphology of the arcs emerging from the emission-line source and could explain the elongated and extended nature of the Hα source. If the emission-line source is lensed, its intrinsic luminosity would be reduced by a substantial factor from that estimated from its observed infrared flux.

We obtained new infrared and optical spectroscopic observations of both the emission-line object (hereafter referred to as the southern source) and the close companion (hereafter referred to as the northern source) in FSC 10214+4724 to further probe this most interesting source using the near-infrared camera and the low-resolution imaging spectrograph on the W. M. Keck Telescope. The new observations reported here add further support to the picture of an AGN origin for the bulk of the observed luminosity and show that there must

be several environments being viewed through different amounts of extinction.

2. OBSERVATIONS AND DATA REDUCTION

The infrared observations reported here were obtained on the nights of 1994 May 1 and 3 on the W. M. Keck Telescope using the grism mode of the near-infrared camera. The instrument, described by Matthews & Soifer (1994), uses a long slit in the focal plane of the telescope, coupled with a grism and bandpass filter. The resolution of the spectrum, with a 0″.7 slit width, is $\lambda/\Delta\lambda \sim 80$. The observations were obtained with a 38″ × 0″.7 slit at a position angle of 0°, so that both the southern and northern sources (Soifer et al. 1992) were observed simultaneously. The seeing was $\simeq 0″.8$. Spectra spanning the wavelength ranges 1.0–1.6 μm and 1.4–2.4 μm were obtained separately. Each set of spectra consisted of a series of observations obtained with the objects at different positions along the slit to facilitate sky subtraction. Individual integrations were 60 or 90 s, long enough to be sky background noise–limited at all wavelengths. A total of 30 minutes of integration time was obtained in the 1.0–1.6 μm wavelength range, while 40 minutes of integration time were obtained on the 1.4–2.4 μm spectrum.

Successive spectral frames were differenced to perform first-order sky subtraction. Spectra of the northern and southern sources were then extracted from the difference frames, and the residual sky spectrum was subtracted from the source spectrum in the difference frame. The individual spectra were wavelength-calibrated based on spectra of laboratory and astronomical sources, flat-fielded and flux-calibrated based on spectra of G dwarf stars, and then co-added to produce the final spectra of the objects.

The visual observations consisted of spectra obtained on 1994 March 9–11 with the Keck Telescope using the low-resolution imaging spectrograph (Oke et al. 1994). Two spectra were obtained, each spanning the wavelength range 0.38–0.88 μm, with a 300 lines mm^{-1} grating and a 1″ slit at a position angle of 0°. With a scale of 2.46 Å pixel^{-1} and 5 pixels across the slit in the spectral and spatial domains, the spectral resolution of the optical spectrum is ~ 750 km s^{-1}. The wave-

---

length calibration was obtained from spectra of an argon or neon lamp. The airmass for the spectra was ~1.25. The exposure times were 3000 and 3600 s. Observations of the standard star GD 248, also taken through a 1″ slit, were used to convert the observed spectra of FSC 10214+4724 to flux density.

3. RESULTS

The infrared (rest frame optical) spectrum of the southern source in FSC 10214+4724, plotted as flux density versus wavelength, is presented in Figure 1. The identified emission lines in the spectrum are indicated in the figure. Table 1 contains the equivalent widths and fluxes of these lines relative to Hα. None of the (rest frame) optical emission lines were resolved, leading to a limit on the full width at half-maximum (FWHM) of $\Delta v \leq 3000$ km s^{-1}. The ratio [N II]/Hα was taken from the work of Elston et al. (1994).

The rest frame optical spectrum of the southern source is rich in the emission lines expected in AGNs. In agreement with the observations of Soifer et al. (1991, 1992) and Elston et al. (1994), the lines of Hα + [N II] and [O III] are seen to be quite strong. The present observations show that other strong lines expected in AGNs are also present. All of the strongest lines identified in the spectrum of Cygnus A (Osterbrock 1989, p. 320) that are accessible in the atmospheric windows appear to be present in this spectrum. What is most unusual about the observed spectrum is the apparent strength of the rest frame UV lines of [Ne III] 3869 Å and [Ne V] 3345 Å, 3426 Å and the weakness of the [O II] 3727 Å line.

The low-dispersion visual (rest frame UV) spectrum of the southern emission line source is displayed in Figure 2. In addition to the strong emission lines of N V, C IV, He II, C III], and Ne IV previously reported by Rowan-Robinson et al. (1991, 1993) and Elston et al. (1994), many weaker lines are clearly present. These range from low-excitation lines such as N II and Si II to moderate excitation lines such as O IV] + Si IV. Lyα is clearly present, though its peculiar profile and weakness relative to N V are abnormal for AGNs. The profile of Lyα is repeatable in the various spectra obtained, and so is quite reliable. The double-peaked profile of Lyα suggests that it is significantly self-absorbed. There is a weak, unidentified line
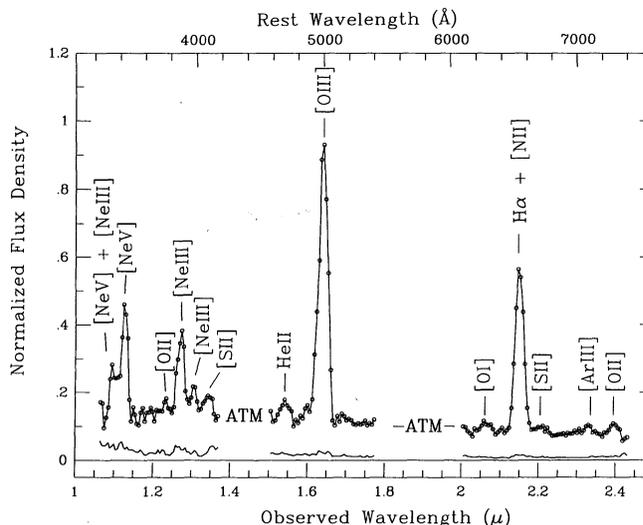

FIG. 1.—The near-infrared (rest frame optical) spectrum of the emission-line (southern) source in FSC 10214+4724. The points represent the flux density per unit wavelength interval, plotted vs. wavelength; the thin line represents the uncertainties in the measured flux density, plotted vs. wavelength. The observed wavelengths are plotted along the bottom, while the rest frame wavelengths are plotted on the top. The regions of strong atmospheric opacity are omitted from the plot. All of the strong emission lines are indicated.

that is blended with C III]. Table 2 reports the equivalent widths, measured FWHM and fluxes for the identified lines in the rest frame UV spectrum. The FWHM was determined from the best-fit single Gaussian to the line profile and has had the instrumental resolution removed. The widths of the (rest frame) ultraviolet lines are as large as FWHM ~ 1700 km s^{-1}, which is greater than values generally associated with Seyfert 2 nuclei.

We obtained spectra of the northern source in the infrared (rest frame optical) and optical (rest frame ultraviolet). These are of significantly lower signal-to-noise ratio than the spectra presented in Figures 1 and 2, and no spectral features, either lines or continuum breaks, that can confidently be associated

TABLE 1
OBSERVED STRENGTHS OF REST FRAME OPTICAL EMISSION LINES

Rest Wavelength (μm)	ID	Observed Wavelength (μm)	Equivalent Width[a] (μm)	R[b]
0.3346	[Ne V]	1.094	$2.0 \pm 0.6 \times 10^{-2}$	0.36 ± 0.13
0.3426	[Ne V]	1.127	$6.2 \pm 0.6 \times 10^{-2}$	1.17 ± 0.20
0.3727	[O II]	1.232	$3 \pm 2 \times 10^{-3}$	0.07 ± 0.05
0.3869	[Ne III]	1.272	$4.3 \pm 0.3 \times 10^{-2}$	0.88 ± 0.15
0.3967	[Ne III]	1.301	$1.2 \pm 0.3 \times 10^{-2}$	0.25 ± 0.08
0.4072	[S II] + Hδ	1.337	$8.5 \pm 3.2 \times 10^{-3}$	0.18 ± 0.07
0.4686	He II	1.541	$9.9 \pm 2.6 \times 10^{-3}$	0.20 ± 0.06
0.4990	[O III]	1.640	$2.0 \pm 0.3 \times 10^{-1}$	4.50 ± 0.64
0.6300	[O I]	2.067	$8.5 \pm 2.3 \times 10^{-3}$	0.14 ± 0.04
0.6562	Hα + [N II]	2.149	$1.63 \pm 0.03 \times 10^{-1}$	
	Hα		$6.5 \pm 0.9 \times 10^{-2}$	1.00 ± 0.14[c]
	[N II]		$9.8 \pm 1.4 \times 10^{-2}$	1.50 ± 0.21[c]
0.6724	[S II]	2.202	$8.5 \pm 2.3 \times 10^{-3}$	0.13 ± 0.04
0.7136	[Ar III]	2.330	$5.9 \pm 2.0 \times 10^{-3}$	0.09 ± 0.03
0.7325	[O II]	2.399	$1.4 \pm 0.4 \times 10^{-2}$	0.18 ± 0.06

[a] Observed.
[b] $R = F(\text{line})/F(\text{H}\alpha)$.
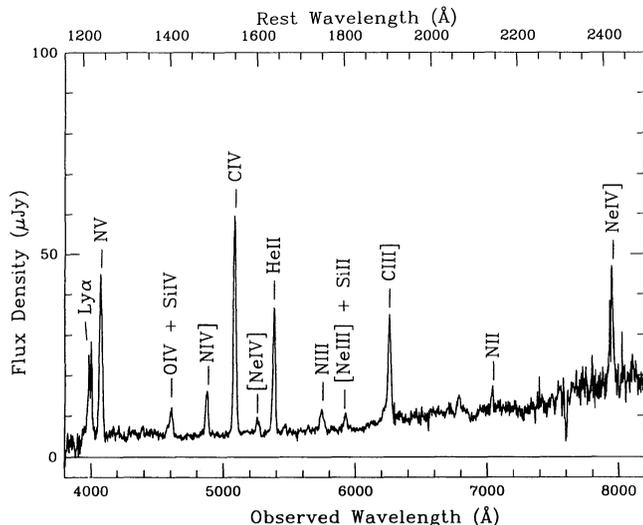[c] From Elston et al. 1994.

FIG. 2.—The optical (rest frame ultraviolet) spectrum of the emission-line source in FSC 10214+4724. The flux density is plotted vs. wavelength. The observed wavelengths are plotted along the bottom, while the rest frame wavelengths are plotted on the top. The identified emission lines are indicated in the plot.

with the object are apparent. Weak emission lines at the wavelengths of the observed lines of [O III] and Hα in the southern source are present in the spectrum of the northern source, but because these lines are quite bright in the southern source, it is likely that they are simply spillover from the southern source. Thus the present observations cannot address the question of whether the northern source is indeed at the same redshift as the southern source or is an intervening gravitational lens. With somewhat better seeing, such observations would be quite feasible on the Keck Telescope.

4. DISCUSSION

The rest frame visual/UV spectrum of FSC 10214+4724 shows emission lines from a wide range of elements and ionization states, ranging from [O I] 6300 Å to [Ne V] 3345 Å, 3426

Å. The detection of the Ne V lines demonstrates the presence of 100 eV ionizing photons, thereby giving strong support to the picture that a substantial fraction of the luminosity in this source originates in a nonstellar source, i.e., an AGN.

The strong far-infrared emission suggests that this source is dusty and possibly heavily obscured, which is consistent with the lack of detection of broad hydrogen recombination lines. This picture of a highly obscured power source is supported by the large Hα/Hβ ratio found by Elston et al. (1994), which suggests $A_v > 5$ mag.

The simple picture of a highly obscured AGN is not, however, consistent with the observations of this source. Qualitatively, the mere detection of the UV lines (Elston et al. 1994) is inconsistent with the model that the entire emission-line region is viewed through >5 mag of visual extinction. In addition, the observed strong polarization of the rest UV spectrum drops substantially to the rest frame optical (Jannuzi et al. 1994), suggesting that the UV light is scattered from a polarizing dust cloud, and that different physical regions contribute to the observed spectrum.

The detection of the He II 4686 Å recombination line (Fig. 1) along with the 1640 Å line reported here and by Elston et al. permits the determination of the reddening between these wavelengths. The observed ratio of the 1640 Å and 4686 Å lines, ∼1.3, corresponds to a reddening $E(1640$ Å–4686 Å$)$ of 1.8 mag, or a visual extinction of ∼1.1 mag. The visual extinction inferred from the apparent Lyα/Hα line ratio is also 1.5 mag, if an intrinsic line ratio inferred from case B recombination theory is assumed (Osterbrock 1989). This is an upper limit to the reddening, since the intrinsic Lyα/Hα ratio could be substantially less than that of case B (Osterbrock).

Further evidence for a multiple component model comes from the line strengths in the observed spectrum. Reddening-insensitive emission-line flux ratios in the observed spectrum were compared with those calculated using the CLOUDY program (Ferland 1991) and found to be inconsistent with a single set of model parameters. A series of models was run with a fixed AGN input ionizing spectrum as characterized by Mathews & Ferland (1987) and Engargiola et al. (1988). The electron density was varied between 10^2 and 10^6 cm^{-3}, and the ionization parameter (photon flux divided by electron density)

TABLE 2

OBSERVED STRENGTHS OF REST FRAME ULTRAVIOLET EMISSION LINES

Rest Wavelength (μm)	ID	Observed Wavelength[a] (μm)	Equivalent Width[b] (μm)	FWHM[c] (km s^{-1})	Flux (10^{-16} ergs cm^{-2} s^{-1})
0.1216	Lyα	0.3990	1.00×10^{-2}		11.5 ± 1.7
0.1240	N V	0.4071	1.66×10^{-2}	1740	18.6 ± 2.8
0.1402	O IV] + Si IV	0.4605	5.3×10^{-3}		3.3 ± 0.5
0.1486	N IV]	0.4876	4.8×10^{-3}	1410	3.2 ± 0.5
0.1549	C IV	0.5084	2.45×10^{-2}	1270	15.1 ± 2.2
0.1601	[Ne IV]	0.5255	1.6×10^{-3}		0.8 ± 0.3
0.1640	He II	0.5383	1.24×10^{-2}	890	7.2 ± 1.1
0.1750	N III	0.5740	2.3×10^{-3}	1480	1.8 ± 0.3
0.1804	Si II + [Ne III]?	0.5922	1.7×10^{-3}		1.0 ± 0.3
(0.1896)......	?	0.6221	1.5×10^{-3}		0.9 ± 0.3
0.1909	C III]	0.6262	7.1×10^{-3}	965	4.9 ± 0.7
(0.2068)......	?	0.6785	1.4×10^{-3}		0.8 ± 0.3
0.2140	N II?	0.7040	1.0×10^{-3}		0.5 ± 0.3
0.2424	Ne IV]	0.7953	5.2×10^{-3}	825	3.8 ± 0.6

[a] Uncertainty ± 0.0002 μm.
[b] Observed width, uncertainty maximum of $+3$ nm, -2 nm, or 15%.
[c] Uncertainty ± 100 km s^{-1}.

was varied from 10^{-4} to 1. For all models the abundances of the elements were assumed to be solar. CLOUDY assumes a plane parallel geometry.

A comparison of the models with the observations of FSC 10214 + 4724 lead us to infer a wide range of extinctions and physical conditions. The predicted line ratios varied little with electron density but were very sensitive to the ionization parameter. In particular, the observations show strong lines of both low and high ionization, which the models cannot reproduce with a single ionization parameter. The ratios [N II]/Hα (Elston et al. 1994) and [O I] 6300 Å/Hα can be matched with ionization parameters in the range 10^{-3} to 10^{-4}, while the ratios [Ne V] 3426 Å/[Ne III] 3869 Å, and [O II] 3727 Å/[Ne III] 3869 Å are consistent with ionization parameters of 0.1–1. The line ratio [S II] 6713 + 6730 Å/Hα is best fitted with ionization parameters intermediate between these two sets of values. The line ratio [O III]/Hβ, determined by Elston et al. to be > 64 from the lack of detection of Hβ, cannot be fitted by the CLOUDY models at all. This suggests both strong attenuation of the Hβ line, and possibly underlying stellar Hβ absorption. While it is difficult to understand how the higher resolution observations of Hβ by Elston et al. might underestimate its strength, the observed spectrum of FSC 10214 + 4724 in Figure 1 shows an asymmetric profile of [O III] 4959 + 5007 Å, suggesting Hβ contributes to the blue wing of [O III]. If this observation is indeed a detection of Hβ, it would be inconsistent with the observations of Elston et al. but it would be consistent with ionization parameters $> 10^{-2}$.

The observations presented here suggest a picture quite similar to that suggested by Elston et al. (1994) and Jannuzi et al. (1994) where the UV spectrum is seen in scattered light, while the optical spectrum is seen directly. In the rest frame wavelengths below ∼5000 Å the compact high-ionization parameter environment is viewed through a lower reddening column than is the longer wavelength emission.

The reddening-corrected UV flux is not sufficient to directly power the far-infrared luminosity of the source. Correcting the UV/optical continuum for the extinction inferred from the ratio of the He 1640 Å and 4686 Å lines ($A_v \sim 1.1$ mag) gives a power law continuum spectral index of −0.3. Extrapolating this power law to the ionization energy of Ne V accounts for only ∼25% of the infrared luminosity in FSC 10214 + 4724. This fraction is highly uncertain and depends critically on the reddening and the assumption that the power law extends uniformly to ∼100 eV. If, however, the mean UV flux is affected by greater extinction than determined from the helium lines, or if the observed UV flux is scattered light from a cloud subtending a small solid angle as viewed from the source, or if the

mean UV albedo of the reflecting cloud is substantially less than 1, the UV continuum would readily account for the bulk of the infrared luminosity. Alternatively, extrapolating this power law to X-ray energies can account for the total bolometric luminosity and remain consistent with the upper limit on the X-ray flux at 3.3 keV (Lawrence et al. 1994).

The (rest frame) visual observations are consistent with the picture of the emission lines originating in a large "narrow-line region" more distant from the ionizing source than the gas producing the UV lines. The extended Hα source is likely produced in a region even larger than the narrow-line region. A low-ionization parameter environment is contributing substantially to the observed spectrum at wavelengths longer than 5000 Å. The [N II]/Hα and [O I]/Hα ratios are inconsistent with stellar ionization (Stasinska 1990) and lead to substantially lower ionization parameters than the shorter wavelength lines. The line ratio [S II]/Hα is consistent with either stellar or nonthermal ionization and an intermediate ionization parameter. The reddening to this region, as determined from the Hα/Hβ line ratio, is significantly greater than inferred from the UV lines.

5. SUMMARY

Based on the observations of the emission lines, we suggest that the ultimate power source of FSC 10214 + 4724 is a dust-enshrouded quasar. The low extinction, high ionization of the UV emission lines coupled with the high extinction, low ionization of the optical emission lines suggests that much of the light below ∼5000 Å in the rest frame is reflected through a region of relatively low extinction into our line of sight, while the longer wavelength radiation is viewed directly through higher extinction.

No spectral features are found in the companion object 1″5 north of the emission-line system. Thus its physical association with the redshift 2.286 system cannot be confirmed.

REFERENCES

Brown, R. L., & Vanden Bout, P. A. 1991, AJ, 102, 1956
Elston, R., McCarthy, P. J., Eisenhardt, P., Dickinson, M., Spinrad, H., Januzzi, B. T., & Maloney, P. 1994, AJ, 107, 910
Engaragiola, G., Harper, D. A., Elvis, M., & Willner, S. P. 1988, ApJ, 332, L19
Ferland, G. J. 1991, OSU Internal Report 91-01
Jannuzi, B. T., Elston, R., Schmidt, G. D., Smith, P. S., & Stockman, H. S. 1994, ApJ, 429, L49
Lawrence, A., Rigopoulou, D., Rowan-Robinson, M., McMahon, R. G., Broadhurst, T., & Lonsdale, C. J. 1994, MNRAS, 266, L41
Mathews, W. G., & Ferland, G. J. 1987, ApJ, 323, L19
Matthews, K., & Soifer, B. T. 1994, in Infrared Astronomy with Arrays: the Next Generation, ed. I. McLean (Dordrecht: Kluwer), 239

Matthews, K., et al. 1994, ApJ, 420, L13
Oke, J. B., et al. 1994, Proc. SPIE, 2198, 178
Odterbrock, D. E. 1989, Astrophysics of Gaseous Nebulae and Active Galactic Nuclei (Mill Valley: University Science Books)
Rowan-Robinson, M., et al. 1991, Nature, 351, 719
Rowan-Robinson, M., et al. 1993, MNRAS, 261, 513
Soifer, B. T., Neugebauer, G., Matthews, K., Lawrence, C., & Mazzarella, J. 1992, ApJ, 399, L55
Soifer, B. T., et al. 1991, ApJ, 381, L55
Solomon, P. M., Downes, D., & Radford, S J. E. 1992, ApJ, 398, L29
Stasinska, G. 1990, A&AS, 83, 501